Electronic Supplementary Material (ESI) for Catalysis Science & Technology.

Supporting Information

The effect of calcium dopant on activity and selectivity of gold catalysts supported on SBA-15 and Nb-containing SBA-15 in methanol oxidation

Joanna Wisniewska*, Izabela Sobczak*, Maria Ziolek

Adam Mickiewicz University, Poznań, Faculty of Chemistry, Uniwersytetu Poznańskiego 8, 61-614 Poznań, Poland

S1 – Syntheses procedures [1,2]

Synthesis of SBA-15 and NbSBA-15 materials

SBA-15 and NbSBA-15 materials were prepared via hydrothermal synthesis, according to a published procedure [1,2]. Pluronic P123 (Poly(ethylene glycol)-block-Poly(ethylene glycol)-block-Poly(ethylene glycol)-block) copolymer was used as a surfactant and TEOS as a source of silicon. The reactant mixture consisted of water, 0.2 M hydrochloric acid (35-38 % HCl, P.O.Ch., Gliwice, Poland), Pluronic P123 (Sigma-Aldrich) and TEOS (Sigma-Aldrich), at the molar ratio: $1SiO_2 : 0.005$Pluronic P123 : $1.45HCl : 124H_2O$. After dissolving Pluronic P123 in HCl solution, the source of silica was added. The mixture was stirred at 310 K for 20 h, moved into a PP bottle and heated without stirring at 373 K for 24 h. The solid was filtered, washed with deionized water and dried at 333 K for 12 h. The template was removed by calcination at 773 K for 8 h in air in static conditions (temperature rate 6 K min^{-1}). For the preparation of NbSBA-15 material, $C_4H_4NNbO_9$ x H_2O (Sigma-Aldrich) was added to the synthesis gel 5 min after TEOS addition. The nominal Si/Nb was 40.

S2 – Characterization techniques [3–5]

ICP-OES

The inductively coupled plasma optical emission spectrometer (ICP-OES) ICPE-9820 (Shimadzu, Japan) with a mini-torch was used for qualitative and quantitative detection of selected elements in studied samples. Before the analysis, about 100 mg of a sample studied and 4 mL H_2O, 3 mL H_2SO_4, 3 mL H_3PO_4 and 2 mL HF (all reagents were for trace analysis, Sigma Aldrich, USA) were added to a teflon tube and mineralized in Microwave oven (Anton Paar, Austria) in three steps: ramp time 5 min. (1500 W), hold time 50 min. (1500 W) and cooling to 343 K.

X-ray diffraction (XRD)

XRD measurements were carried out on a Bruker AXS D8Advance diffractometer with Cu K_α radiation (λ= 0.154 nm), with a step size of 0.05° in the small-angle range (1°–10°) and with a step size of 0.2° in the wide-angle range (20°–70°). The measurements were performed for samples pretreated in the flow of argon (40 mL/min) for 2 h at 623 K and after methanol oxidation.

N_2 adsorption/desorption isotherms

The N_2 adsorption-desorption isotherms were obtained at 77 K using a Micromeritics ASAP 2020 Physisorption Analyzer. Before measurements, the samples were degassed at 573 K for 8 h. The surface area was calculated by the BET method, whereas the volume and diameter of pores were determined by the DFT method. The micropore volume were determined by the t-plot method.

UV–vis spectroscopy

UV–vis spectra were recorded using a Varian-Cary 300 Scan UV–visible spectrophotometer. Powder samples were placed in a cell equipped with a quartz window. The spectra were recorded in the range from 800 to 190 nm. Spectralon was used as the reference material. The measurements were performed for samples pretreated in the flow of argon (40 mL/min) for 2 h at 623 K and after methanol oxidation.

X-ray Photoelectron Spectroscopy (XPS)

X-ray Photoelectron Spectroscopy (XPS) was performed on an Ultra-high vacuum photoelectron spectrometer based on Phoibos150 NAP analyzer (Specs, Germany). The analysis chamber was operated under vacuum with a pressure close to 5×10^{-9} mbar and the sample was irradiated with a monochromatic $Al_{K\alpha}$ (1486.6 eV) radiation (15 kV; 10 mA). Spectra were recorded with a flood gun acting as neutralizer. Binding energies were referenced to the Si 2p peak from silica 103.4 eV. The measurements were performed for as-made catalysts, for samples pretreated in the flow of argon (40 mL/min) for 2 h at 623 K and after methanol oxidation.

Test reaction - 2-propanol decomposition

The 2-propanol dehydration and dehydrogenation was performed using a microcatalytic pulse reactor inserted between the sample inlet and the column of a CHROM-5 chromatograph. A portion of 0.05 g of the granulated catalyst was activated at 623 K for 2 h under helium flow (40 mL/min). The 2-propanol (Chempur Poland) conversion was studied at 523 K using 3 μl pulses of alcohol under helium flow (40 mL/min). The substrate was vaporized before being passed through the catalyst bed with the flow of helium carrier gas. The products such as propene, 2-propanone (acetone) and diisopropyl ether were identified by SRI chromatograph online with a microreactor. The reaction mixture was separated on a 2-m column filled with Carbowax 400 loaded on Chromosorb W (80–100 mesh) at 363 K in helium flow (40 mL/min) and detected by TCD.

S3 – Methanol oxidation [3,6]

Granulated catalyst (0.02 g) of the size fraction of $0.5 < \phi < 1$ mm was placed into a tubular reactor (diameter $\Phi = 5$ mm, length $l = 70$ mm). The temperature was controlled by a thermocouple located in the catalyst bed (6-7 mm height). The samples were activated in argon flow (40 mL/min) at 623 K for 2 h (with a ramp of 15 K/min). The reactant mixture of $Ar/O_2/CH_3OH$ (88/8/4 mol %) was flowing through the reactor at the rate of 40 mL/min. The external (checked by tests with the use of different volumes of catalysts and constant granular size of catalysts and contact time) and internal (monitored by tests with the use of different granular sizes of catalyst and constant volume of catalyst and contact time) diffusion do not limit the reaction rate in these conditions. Methanol (Chempur, Poland) was introduced to the flow reactor by bubbling argon gas through a glass saturator filled with methanol. The outlet stream line from the reactor to the gas chromatograph was heated at about 373 K to avoid condensation of the reaction products. The reactor outflow was analyzed using two online gas chromatographs in which argon was used as a carrier gas. One gas chromatograph, GC 8000 Top, was equipped with a capillary column of DB- 1, operated at 313 K, and a FID detector applied for analyses of organic compounds, while the other GC containing Porapak Q and 5A molecular sieves columns (used for analyses of O_2, CO_2, CO, H_2O, and CH_3OH) had a TCD detector. The selectivity, S_i, was calculated as the molar concentration of the particular product (i) divided by the sum of the concentrations of all products detected, $S_i = c_i / \sum c \times 100$ %. The following products detected by FID and TCD detectors were analyzed: methanol, formaldehyde, methyl formate, dimethoxymethane, dimethyl ether and carbon dioxide. The product distribution was illustrated by selectivities and yields.

S4 - Characterization of catalysts after oxidation of methanol

To characterize changes in the oxidation states of metal components after methanol oxidation, the catalysts were subjected to XPS and UV-vis spectroscopy examination. Figure 1 displays the UV-vis spectra before and after methanol oxidation. No significant changes in positions of the main absorption bands can be noticed, which proves high stability of gold species in the prepared samples. Figures S8-S13 display the XP spectra of the studied catalysts in Au 4f, Ca 2p, Nb 3d, Si 2p, O 1s and C 1s regions, whereas Table 3 presents the XPS bands positions. As can be seen from Table 3, Figures S8 and S9, the positions of XP bands assigned to gold and calcium did not change after methanol oxidation. Gold (similarly as before methanol oxidation) was exclusively present as negatively charged metallic species $(Au^0)^{\delta-}$, characterized by XPS bands at BE $4f_{7/2}$ = 83.1 and 83.3 eV, confirming its high stability upon reaction conditions. In Ca 2p region, the bands at BE = 347.1 – 347.4 eV (Ca $2p_{3/2}$) and at BE = 350.8 – 351.1 eV (Ca $2p_{1/2}$) were assigned to Ca^{2+} species which could be present in calcium carbonate ($CaCO_3$) or calcium oxide (CaO).

The XPS spectra in Nb 3d region (Fig. S10) indicate that Nb in all samples after methanol oxidation was present exclusively as Nb^{5+} species. Similarly as before the catalytic reaction, the binding energy of Nb $3d_{5/2}$ in Au/Nb_2O_5/SBA-15-R was significantly higher (207.7 eV) than that in the bulk Nb_2O_5 (207.1 eV) [7]. It confirms the interaction of Nb^{5+} with Si within SBA-15 as well as the interaction of small clusters of highly dispersed Nb_2O_5 with the surface of silica. In Au/$CaNbO_x$/SBA-15, the binding energy of Nb $3d_{5/2}$ was significantly lower (206.5 eV) than that in the bulk Nb_2O_5 (207.1 eV). It suggest the interaction between niobium and other catalysts components (calcium and/or gold) or the interaction with chemisorbed products and intermediates.

Analysis of silicon spectra in Si 2p region (Fig. S11) showed no significant changes for almost all catalysts. Silicon in Si-O-Si bonds (Si_{II}) dominated in all samples and gave XP band at 103.4 eV. For Au/Ca/SBA-15-R, Au/NbSBA-15-R and Au/Ca/NbSBA-15-R catalysts an additional band at BE = 102.4 – 102.7 eV appeared, which proves the presence of defects generated by calcium (Si-O-Ca) and/or niobium (Si-O-Nb) modification [8]. Interestingly, this band did not appear after deconvolution of Au/CaNbO$_x$/SBA-15-R spectrum, although it was present in the spectrum of this sample before the catalytic reaction. It is possible that defects in silica support generated by calcium were occupied by substrate or intermediate products of methanol oxidation.

Interesting results come from analysis of the oxygen and carbon XP spectra (Figs. S12, S13). For three samples (Au/Ca/SBA-15-R, Au/Ca/NbSBA-15-R and Au/Nb_2O_5/SBA-15-R) new species (noted as O_{IV}) characteristic of oxygen in organic compounds (C-O and/or C=O) appeared at BE = 533.2 – 533.6 eV, which confirms the presence of adsorbed organic intermediates and/or products on the surface of these materials. For Au/NbSBA-15 and Au/CaNbO$_x$/SBA-15 catalysts after methanol oxidation the amount of surface hydroxyl groups increased from 13.7 % and 7.4 % to 23.4 % and 31.0 %, respectively. The increase in the number of the surface hydroxyl groups can be related to the abstraction of hydrogen from the adsorbed methanol/reaction products (mainly H_2O) by nucleophilic oxygen species present on the surface of the catalysts. For all samples (except for Au/SBA-15-R) the XPS spectra in C1 region displayed two bands. The main band was located at BE = 284.3- 284.6 eV and was assigned to residual template used for synthesis of the support. In the spectra of Au/NbSBA-15-R and Au/Ca/NbSBA-15-R, this band was shifted to lower binding energy (284.0 eV). Probably the niobium present in niobiosilicate support affects the interaction with residual organic template. In the spectra of calcium containing samples, after activation, a band at 289.2 eV was observed confirming the presence of $CaCO_3$ species. This band was present in the spectra of Au/Ca/SBA-15 and Au/CaNbO$_x$/SBA-15 catalysts after methanol oxidation. As shown in [9], the signal assigned to carbon in organic species (e.g. Ca(HCOO)$_2$) is shifted to lower binding energy (288.2 eV) in comparison to that of the band coming from CaCO$_3$ (289.0 eV). The shift of XPS band observed for Au/NbSBA-15-R (287.2 eV), Au/Ca/NbSBA-15-R (287.1 eV) and Au/Nb$_2$O$_5$/SBA-15-R (286.4 eV) is even greater and suggests the presence of organic species which probably strongly interact with niobium on the surface of the catalysts.

References

1 D. Zhao, Q. Huo, J. Feng, B. F. Chmelka and G. D. Stucky, *J. Am. Chem. Soc.*, 1998, **120**, 6024–6036.

2 B. Kilos, I. Nowak, M. Ziolek, A. Tuel and J. C. Volta, *Stud. Surf. Sci. Catal.*, 2005, **158 B**, 1461–1468.

3 J. Wisniewska, I. Dziedzic and M. Ziolek, *RSC Adv.*, 2020, **10**, 14570–14580.

4 I. Kaskow, I. Sobczak, C.-M. Yang and M. Ziolek, *Catal. Today*, 2020, **356**, 110–121.

5 J. Wisniewska, K. Grzelak, S. P. Huang, I. Sobczak, C. M. Yang and M. Ziolek, *Catal. Today*, 2020, **356**, 165–177.

6 J. Czaplinska, I. Sobczak and M. Ziolek, *J. Phys. Chem. C*, 2014, **118**, 12796–12810.

7 H. Liu, N. Gao, M. Liao and X. Fang, *Sci. Rep.*, 2015, **5**, 1–9.

8 H. Bala, Y. Zhang, H. Ynag, C. Wang, M. Li, X. Lv and Z. Wang, *Colloids Surfaces A Physicochem. Eng. Asp.*, 2007, **294**, 8–13.

9 B. Demri and D. Muster, *J. Mater. Process. Tech.*, 1995, **55**, 311–314.

Table S1. Texture parameters of studied samples.

Catalyst	BET surface area [m^2g^{-1}]	Total pore volume, DFT [cm^3g^{-1}]	Average pore diameter, DFT [nm]	Micropore volume, t-plot [nm]	Unit cell parameter, XRD [nm]	Average gold particle diameter, from TEM [nm]
SBA-15*	860	1.05	10.7	0.06	11.0	-
Ca/SBA-15*	487	0.67	9.2	0.01	9.9	-
NbSBA-15*	929	1.12	11.5	0.07	11.0	-
Ca/NbSBA-15*	458	0.68	9.6	0.003	10.7	-
Nb_2O_5/SBA-15	532	0.70	9.9	0.03	11.2	-
$CaNbO_x$/SBA-15	902	1.12	9.7	-	11.3	-
Au/SBA-15*	474	0.68	9.6	0.05	10.5	4.9
Au/Ca/SBA-15*	340	0.50	8.3	0.02	10.7	1.8
Au/NbSBA-15*	482	0.65	9.6	0.06	10.5	5.4
Au/Ca/NbSBA-15*	356	0.53	9.4	0.02	10.8	3.0
Au/Nb_2O_5/SBA-15	365	0.53	9.6	0.02	11.2	3.6
Au/$CaNbO_x$/SBA-15	462	0.65	9.6	0.02	10.6	3.0

*Samples characterized in: J. Wisniewska, I. Sobczak, M. Ziolek, *Gold based on SBA-15 supports – promising catalysts in base-free glucose oxidation*, Chem. Eng. J. (2020) DOI: doi.org/10.1016/j.cej.2020.127548.

.

Table S2. Results of methanol oxidation at different temperatures and on different catalysts. Reaction conditions: reagents – $Ar:O_2:CH_3OH$ mol % = 88/8/4 mol %, flow of reactants: 40 mL/min, amount of catalyst – 0.020 g.

Catalyst	Temp. [K]	MeOH conv. [%]	Reaction rate x 10^{-2} $mmol_{MeOH}/g_{kat}$ /min	Selectivity / Yield [%]				
				HCHO	$HCOOCH_3$	CH_3-O-CH_3	CH_2-CH_2	CO_2
Au/SBA-15	473	3	11	8 / 0.2	91 / 3	1 / 0.03	0 / 0	0 / 0
	523	16	57	32 / 5	61 / 10	traces	0	7 / 1
	573	25	89	56 / 14	34 / 9	0	traces	10 / 2
Ca/SBA-15	473	2	7	0	100 / 2	0	0	0
	523	5	18	30 / 2	45 / 2	0	0	25 / 1
	573	11	39	33 / 3	22 / 2	0	0	55 / 6
Au/Ca/SBA-15	373	7	25	100 / 7	0	0	0	0
	423	13	46	100 / 13	0	0	0	0
	473	98	350	0	46 / 45	0	0	54 / 53
	523	100	357	0	0	0	0	100 / 100
	573	100	357	0	0	0	0	100/ 100
NbSBA-15	473	4	14	0	100 / 4.0	0	0	0
	523	9	32	23 / 2	75 / 7	2 / 0.2	traces	0
	573	25	89	26 / 6	55 / 14	1 / 0.25	traces	18 / 4
Au/NbSBA-15	473	8	29	0	100 / 8	0	0	0
	523	17	61	52 / 9	48 / 8	0	0	0
	573	28	100	65 / 18	25 / 7	traces	traces	10 / 3
Ca/NbSBA-15	473	1	4	54 / 0.5	traces	0	0	46 / 0.5

	523	4	14	58 / 2	10 / 0.4	traces	1/ 0.04	31 / 1
	573	7	25	57 / 4.0	21 / 1.5	traces	traces	22 / 1.5
Au/Ca/NbSBA-15	323	0	0	0	0	0	0	0
	373	0.5	2	0	100 / 0.5	0	0	0
	423	4	14	0	100 / 4	0	0	0
	473	98	350	8 / 8	34 / 33	0	0	58 / 57
	523	99	353	22 / 22	6 / 6	0	0	72 / 71
	573	100	355	36 / 36	0	traces	traces	64 / 64
Nb_2O_5/SBA-15	473	3	11	71 / 2	0	15 / 0.5	1 / 0.03	13 / 0.4
	523	6	21	24 / 1	62 / 4	11 / 0.7	traces	3 / 0.2
	573	27	96	33 / 9	54 / 15	9 / 2	traces	4 / 1
Au/Nb_2O_5/SBA-15	423	3	11	0	100 / 3	0	0	0
	473	11	39	23 / 3	66 / 7	traces	0	11/ 1
	523	44	157	35 / 15	39 / 17	1 / 0.4	traces	25 / 11
	573	93	332	40 / 37	8 / 7	4 / 4	2 / 2	46 / 43
Au/$CaNbO_x$/SBA-15	323	1	4	0	100 / 1	0	0	0
	373	4	14	0	100 / 4	traces	0	0
	423	25	89	2 / 0.5	93 / 23	traces	traces	5 / 1
	473	98	350	21 / 20	12 / 12	traces	traces	66 / 65
	523	99	353	45 / 45	5 /5	0	traces	50 / 49
	573	100	355	17 / 17	1 / 1	0	traces	82 / 82

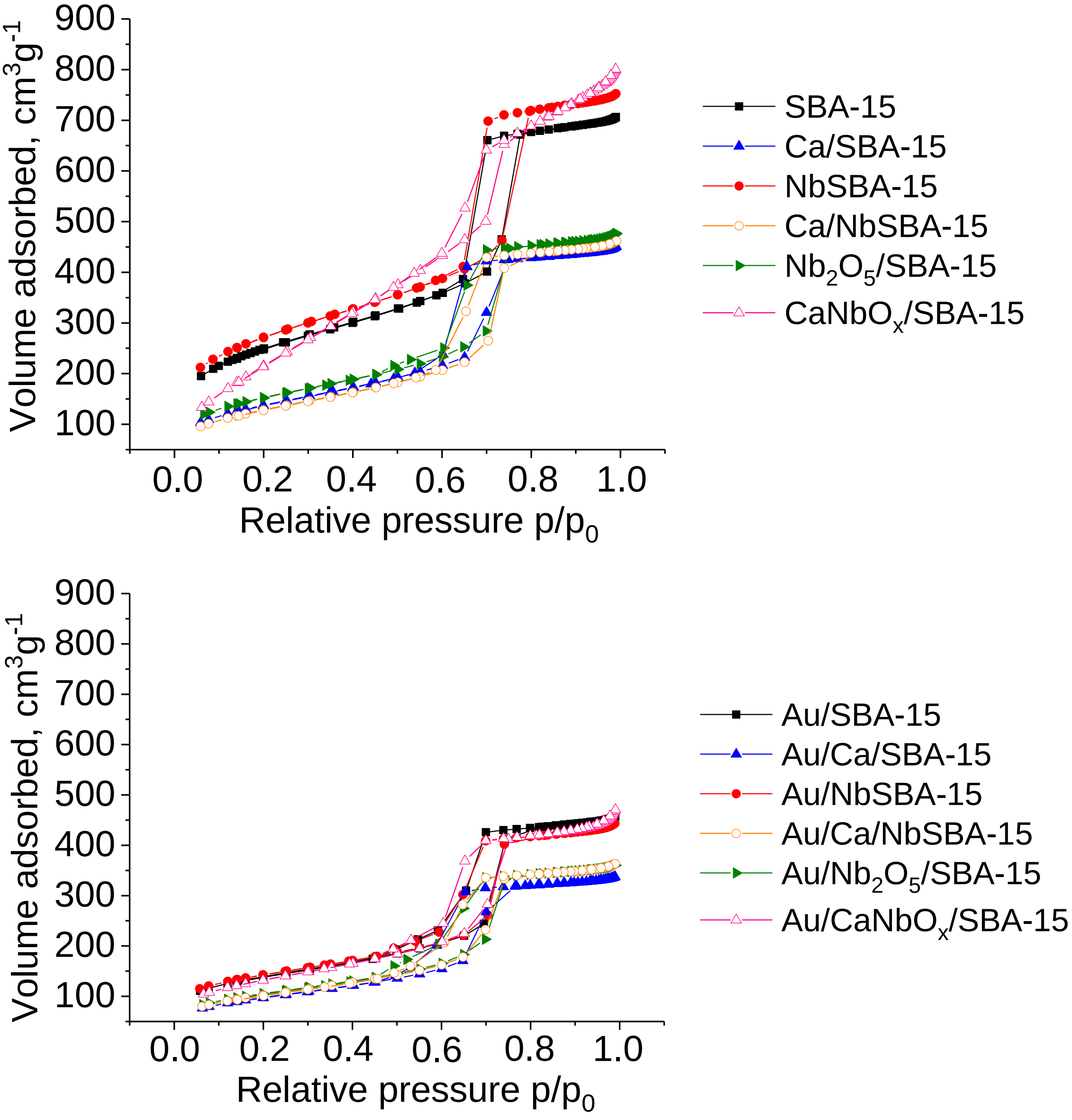

Fig. S1. Nitrogen adsorption/desorption isotherms for supports and gold catalysts.

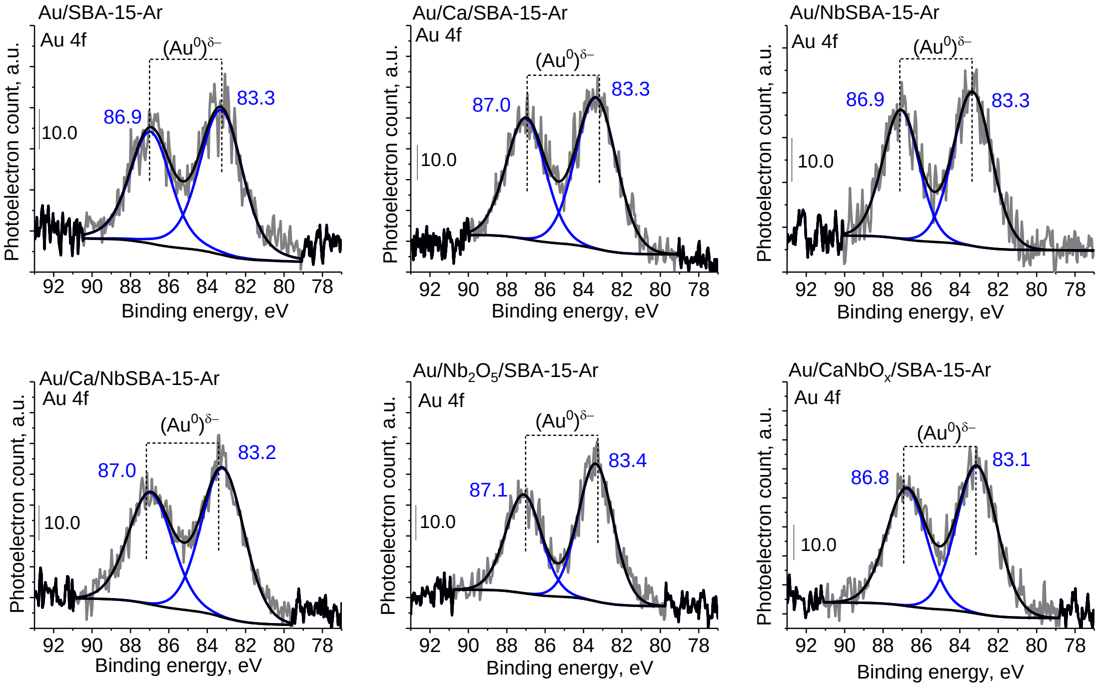
Au/SBA-15-Ar

Au/Ca/SBA-15-Ar

Au/NbSBA-15-Ar

Au/Ca/NbSBA-15-Ar

Au/Nb_2O_5/SBA-15-Ar

Au/$CaNbO_x$/SBA-15-Ar

Fig. S2. XPS spectra of gold catalysts activated at 623 K for 2 h in Ar flow (40 mL/min) – Au 4f region.

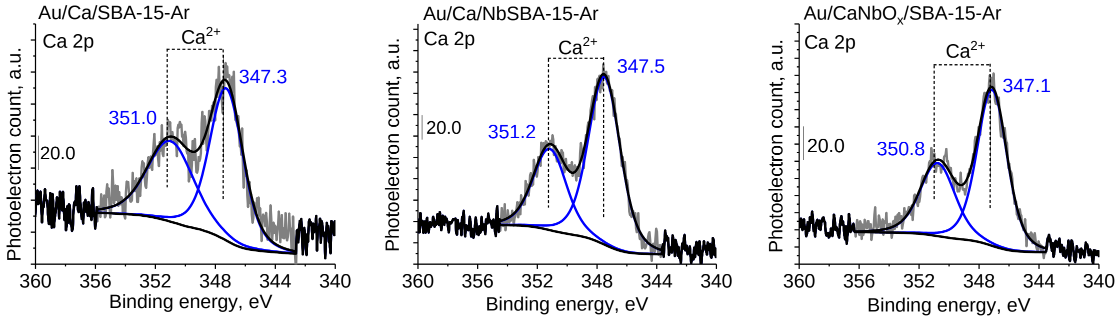

Fig. S3. XPS spectra of gold catalysts activated at 623 K for 2 h in Ar flow (40 mL/min) – Ca 2p region.

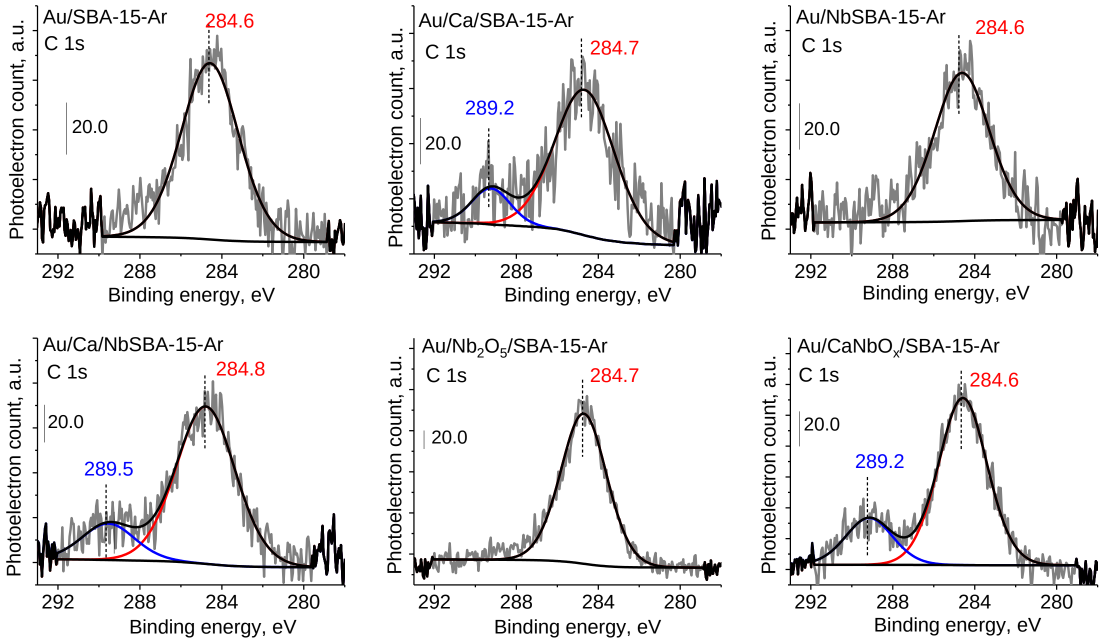

Fig. S4. XPS spectra of gold catalysts activated at 623 K for 2 h in Ar flow (40 mL/min) – C 1s region.

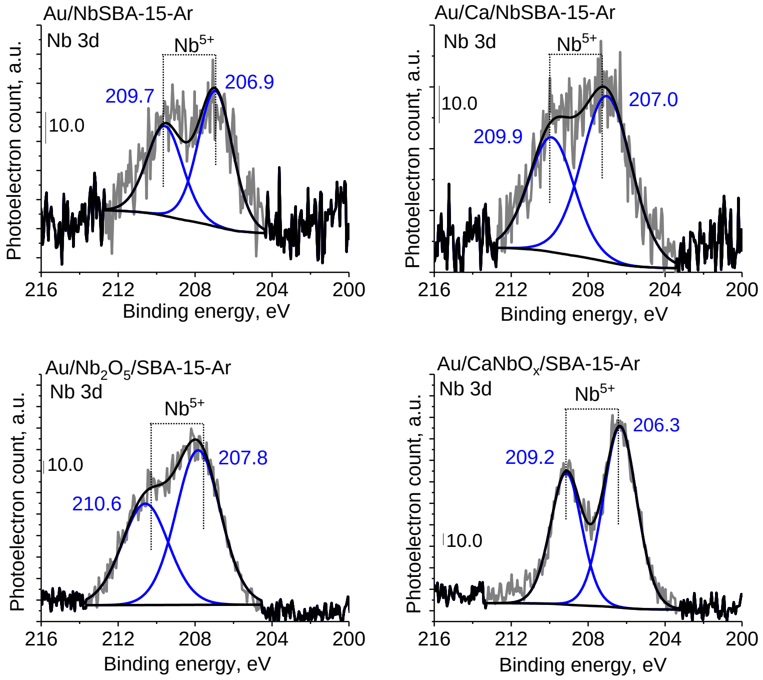

Fig. S5. XPS spectra of gold catalysts activated at 623 K for 2 h in Ar flow (40 mL/min) – Nb 3d region.

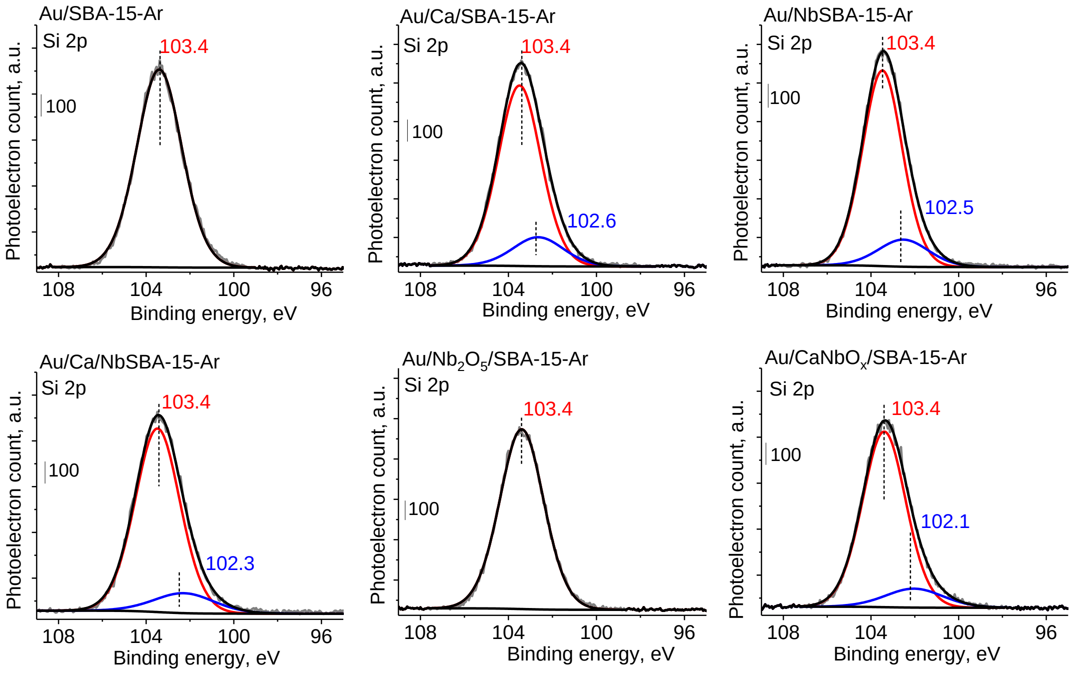

Fig. S6. XPS spectra of gold catalysts activated at 623 K for 2 h in Ar flow (40 mL/min) – Si 2p region.

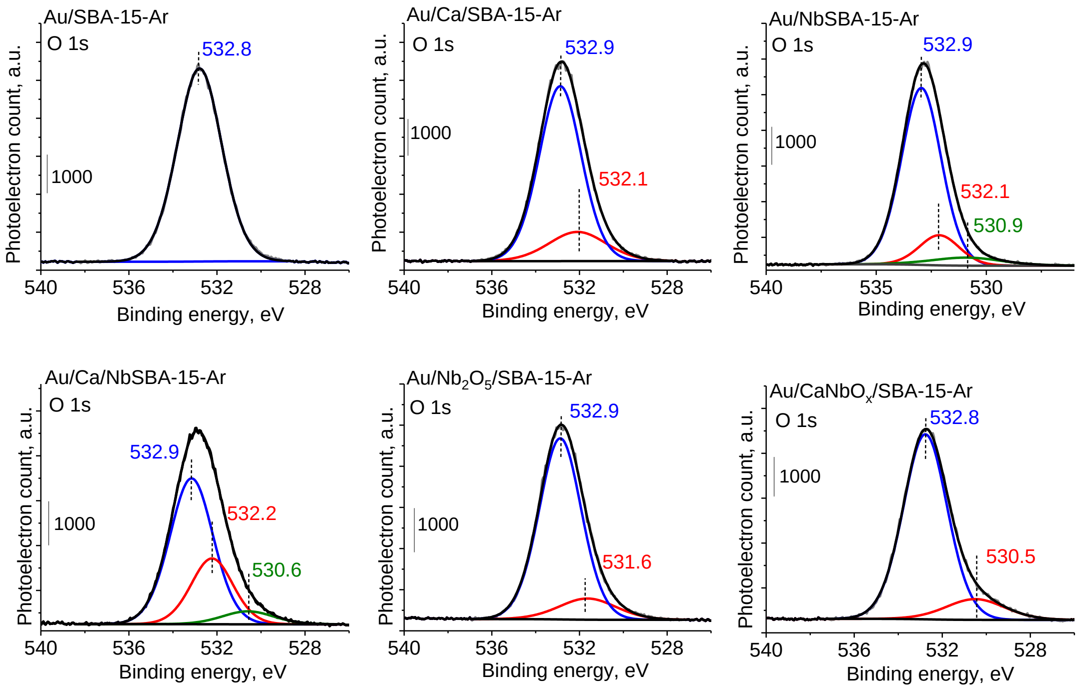

Fig. S7. XPS spectra of gold catalysts activated at 623 K for 2 h in Ar flow (40 mL/min) – O 1s region.

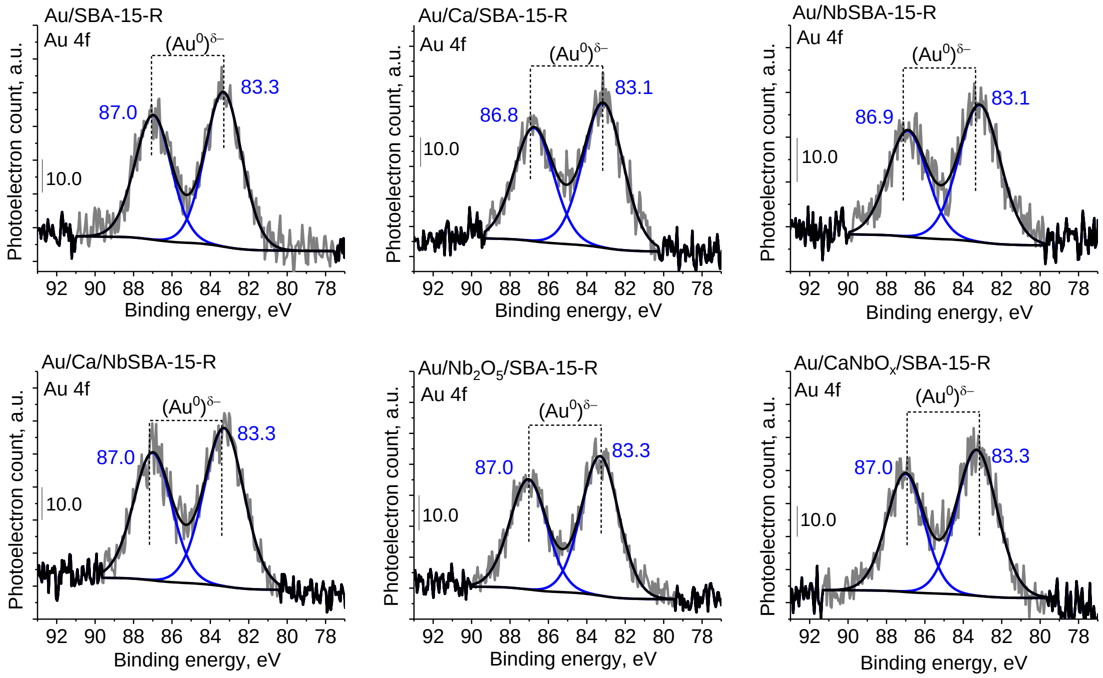

Fig. S8. XPS spectra of gold catalysts after methanol oxidation – Au 4f region. Reaction conditions: reagents – Ar:O$_2$:CH$_3$OH mol % = 88/8/4 mol %, flow of reactants: 40 mL/min, T = 323 K – 573 K, amount of catalyst – 0.020 g.

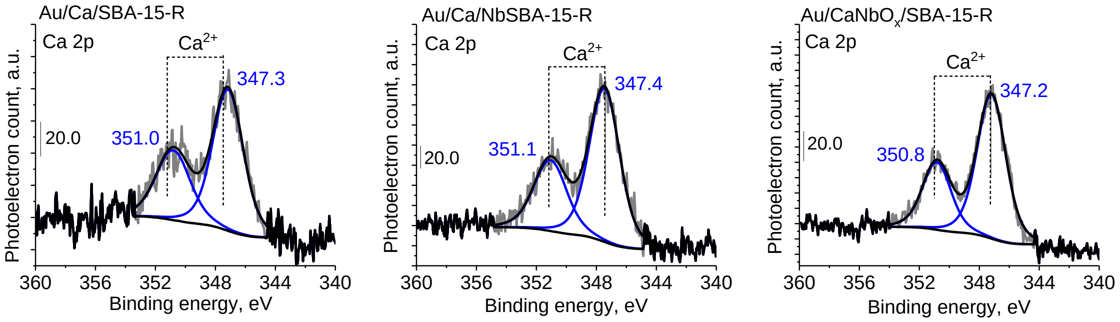

Fig. S9. XPS spectra of gold catalysts after methanol oxidation – Ca 2p region. Reaction conditions: reagents – Ar:O_2:CH_3OH mol % = 88/8/4 mol %, flow of reactants: 40 mL/min, T = 323 K – 573 K, amount of catalyst – 0.020 g.

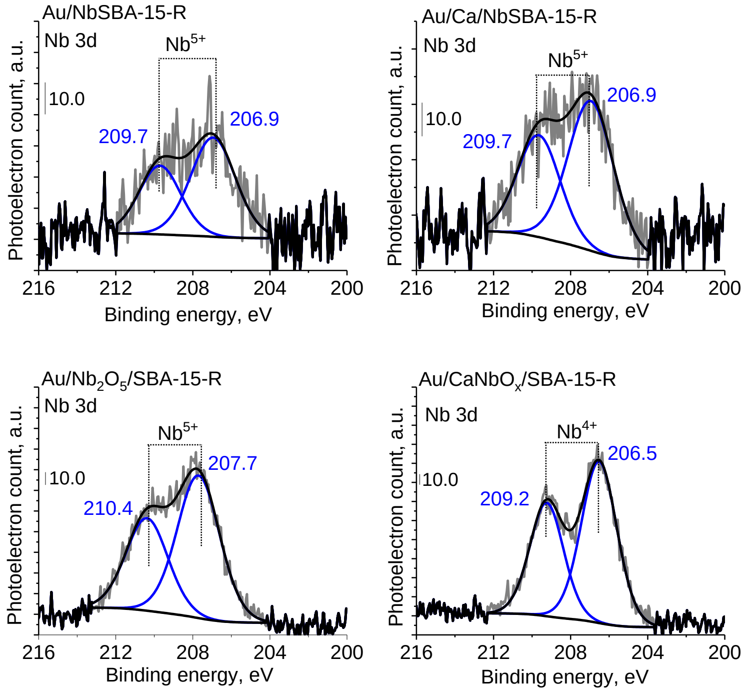

Fig. S10. XPS spectra of gold catalysts after methanol oxidation – Nb 3d region. Reaction conditions: reagents – Ar:O_2:CH_3OH mol % = 88/8/4 mol %, flow of reactants: 40 mL/min, T = 323 K – 573 K, amount of catalyst – 0.020 g.

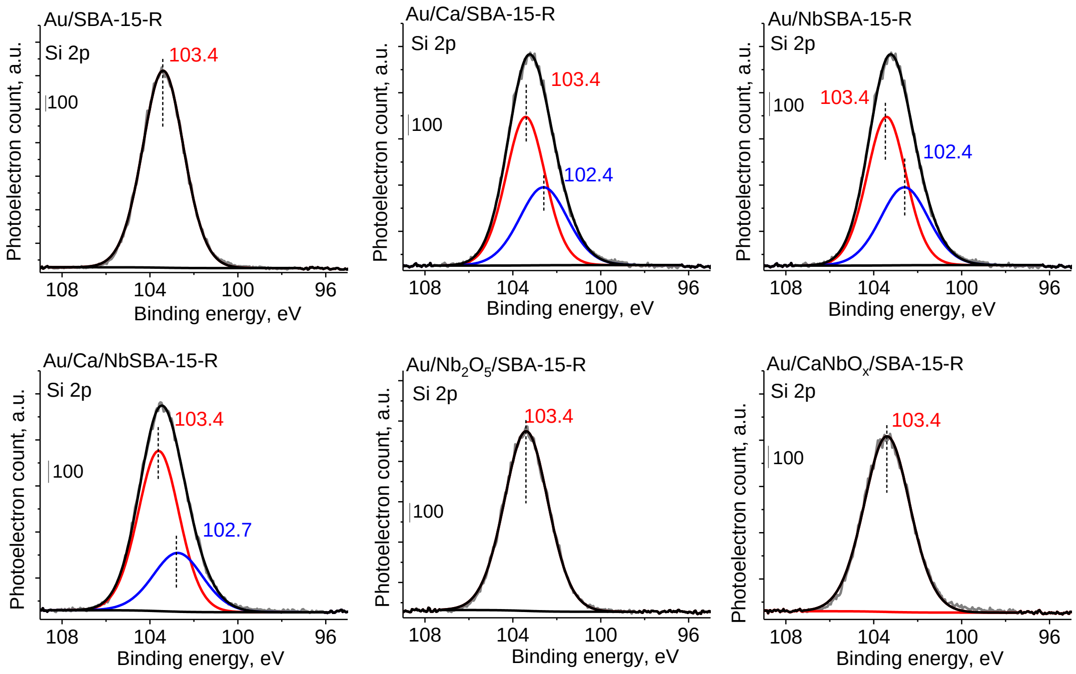

Fig. S11. XPS spectra of gold catalysts after methanol oxidation – Si 2p region. Reaction conditions: reagents – Ar:O$_2$:CH$_3$OH mol % = 88/8/4 mol %, flow of reactants: 40 mL/min, T = 323 K – 573 K, amount of catalyst – 0.020 g.

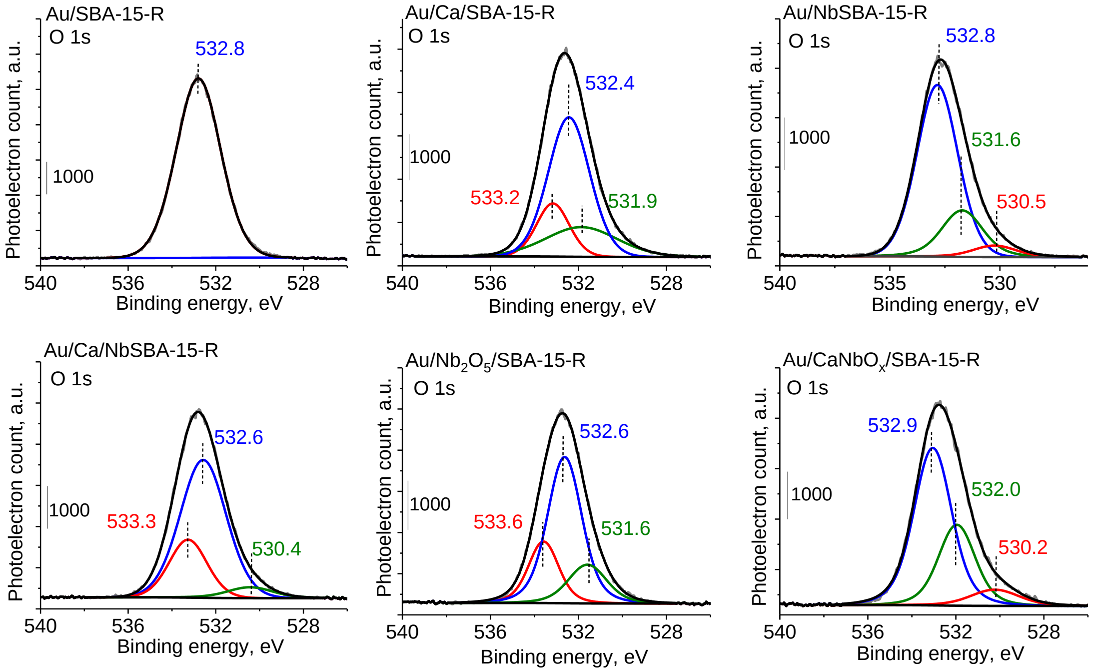

Fig. S12. XPS spectra of gold catalysts after methanol oxidation – O 1s region. Reaction conditions: reagents – Ar:O_2:CH_3OH mol % = 88/8/4 mol %, flow of reactants: 40 mL/min, T = 323 K – 573 K, amount of catalyst – 0.020 g.

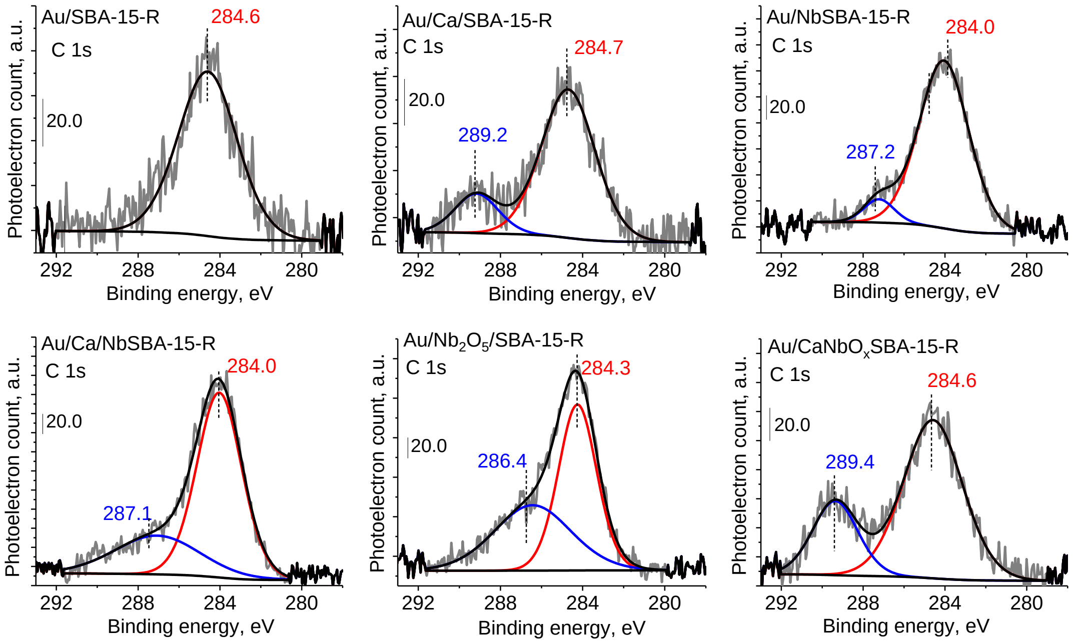

Fig. S13. XPS spectra of gold catalysts after methanol oxidation – C 1s region. Reaction conditions: reagents – Ar:O$_2$:CH$_3$OH mol % = 88/8/4 mol %, flow of reactants: 40 mL/min, T = 323 K – 573 K, amount of catalyst – 0.020 g.

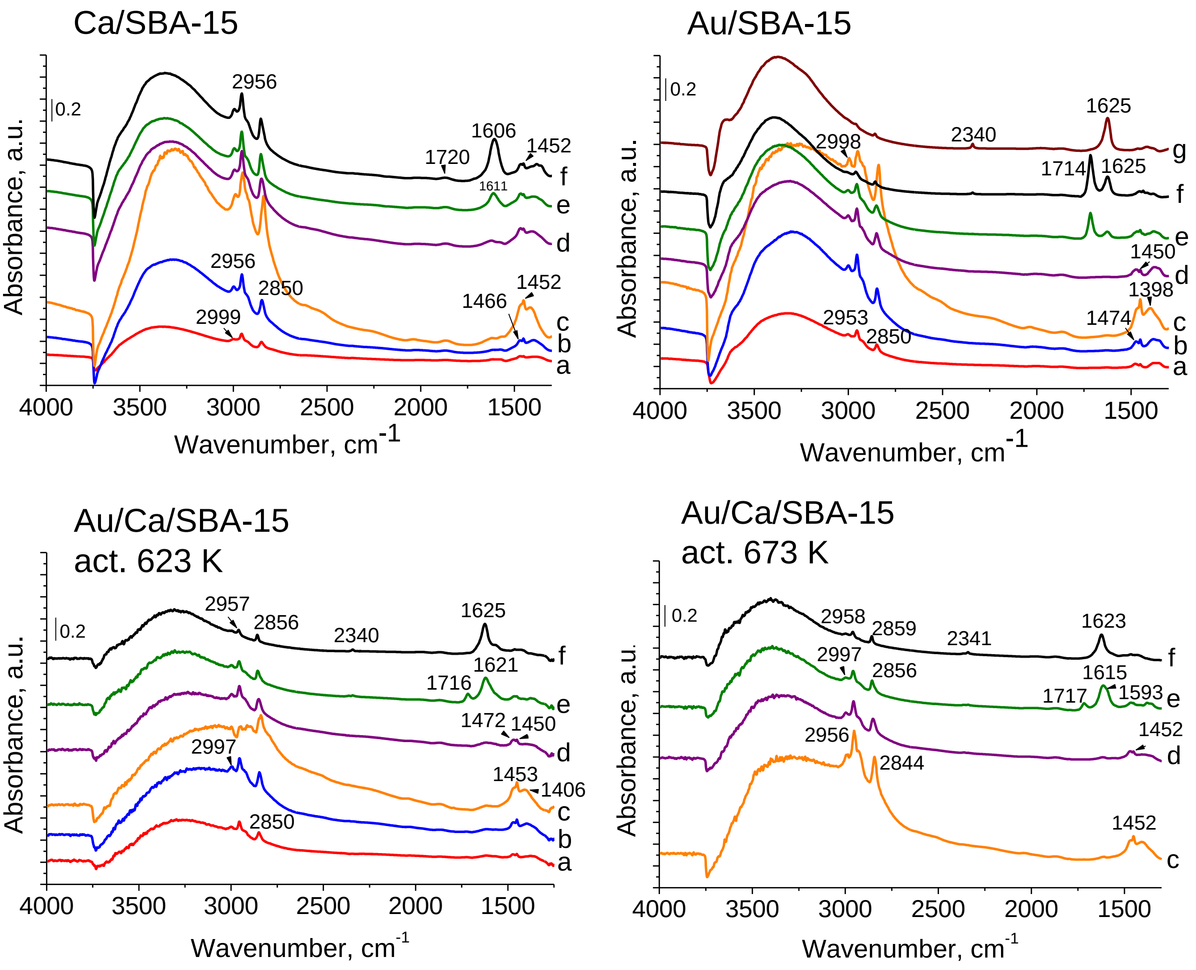

Fig. S14. FTIR spectra (4000-1300 cm^{-1}) of catalysts after MeOH admission at r.t. followed by oxygen introduction and heating at different temperatures: MeOH ads. (1 mbar) (a), MeOH ads. (+1 mbar) (b), MeOH ads. (+ 2 mbar; total = 4 mbar) (c), evacuation for 30 min at r.t. (d), oxygen admission (12 mbar) and heating for 30 min at: 473 K (e), 523 K (f), 573 K (g). The spectra after subtracting of the spectra for activated

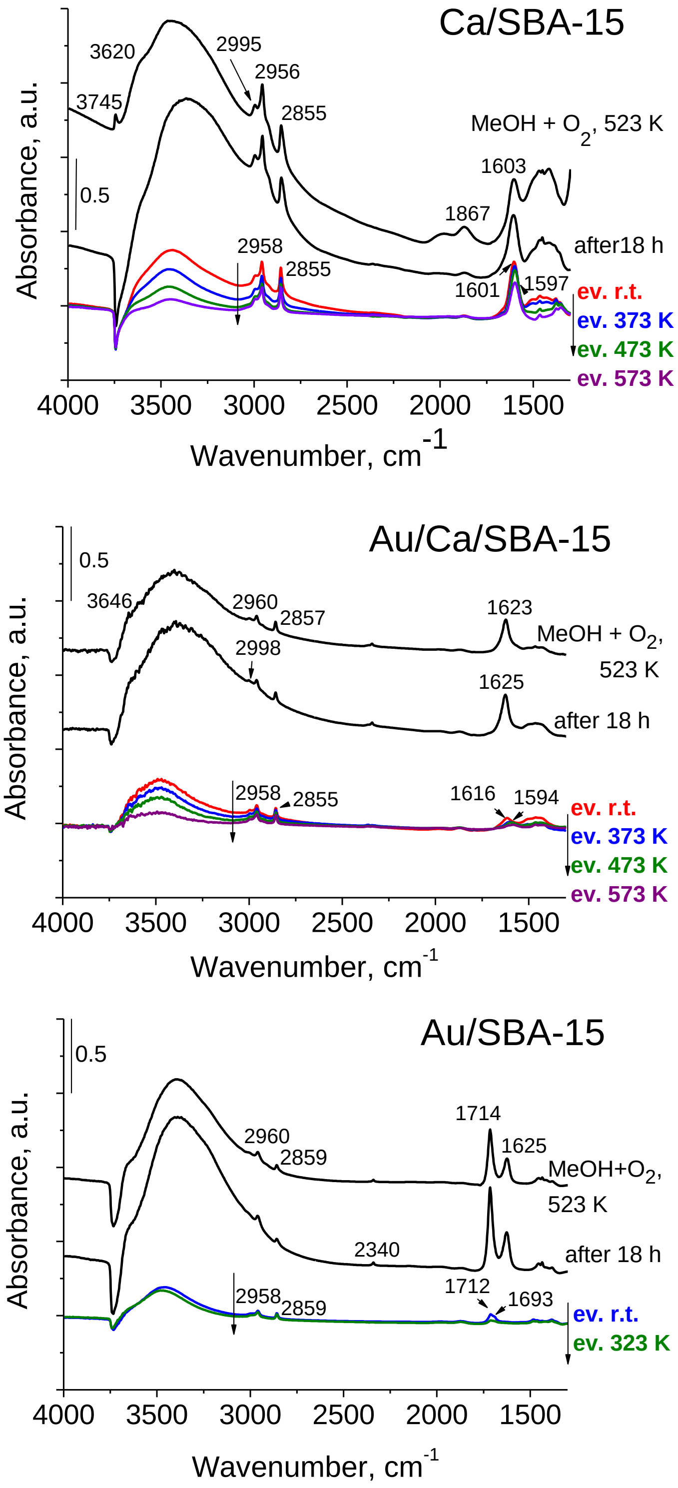

Fig. S15. FTIR spectra of catalysts (4000-1300 cm^{-1}) after adsorption of MeOH (4 mbar) at r.t. followed by short evacuation at r.t.; admission of oxygen (12 mbar) at r.t., heating at 523 K for 30 min and evacuation at different temperatures for 30 min. The spectra after subtracting of the spectra for activated catalysts.

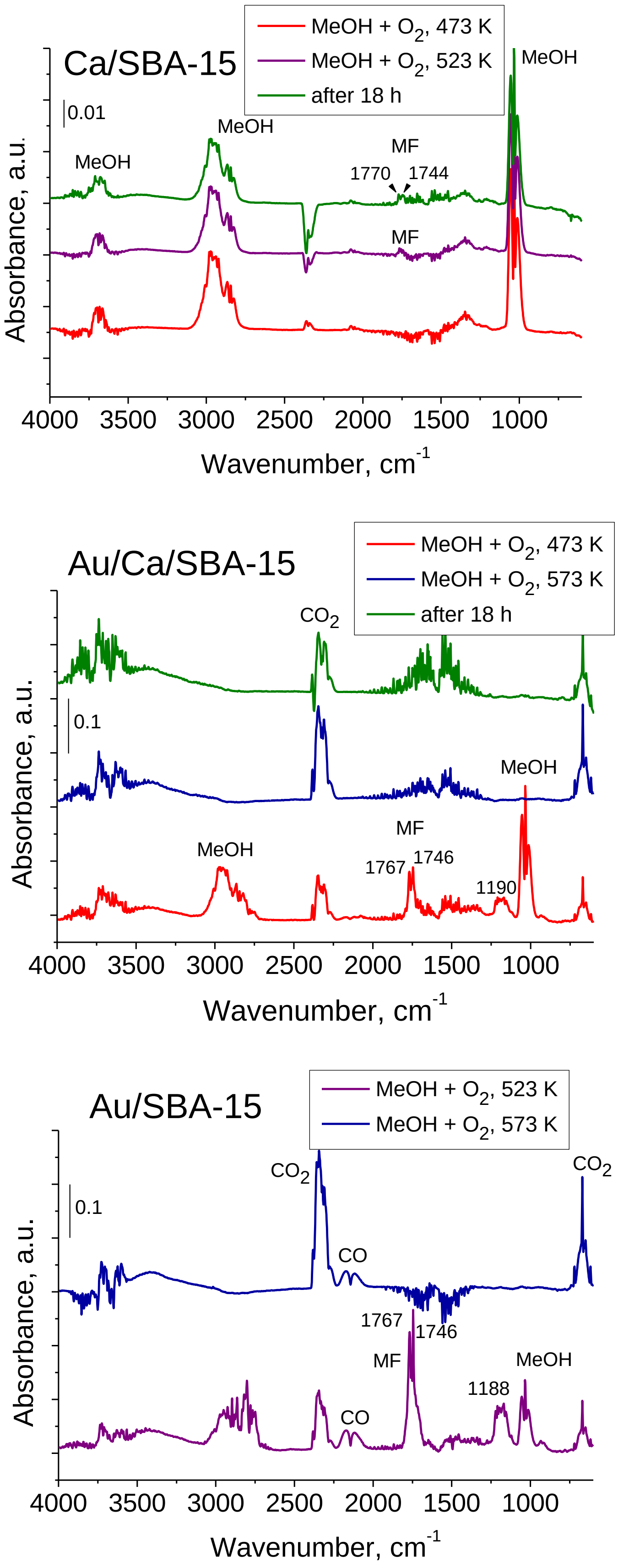

Fig. S16. FTIR spectra of gas phase after MeOH (4 mbar) admission at r.t. followed by short evacuation, oxygen (12 mbar) addition at r.t. and heating of the system at 473 K, 523 K and 573 K for 30 min in the presence of the catalyst.

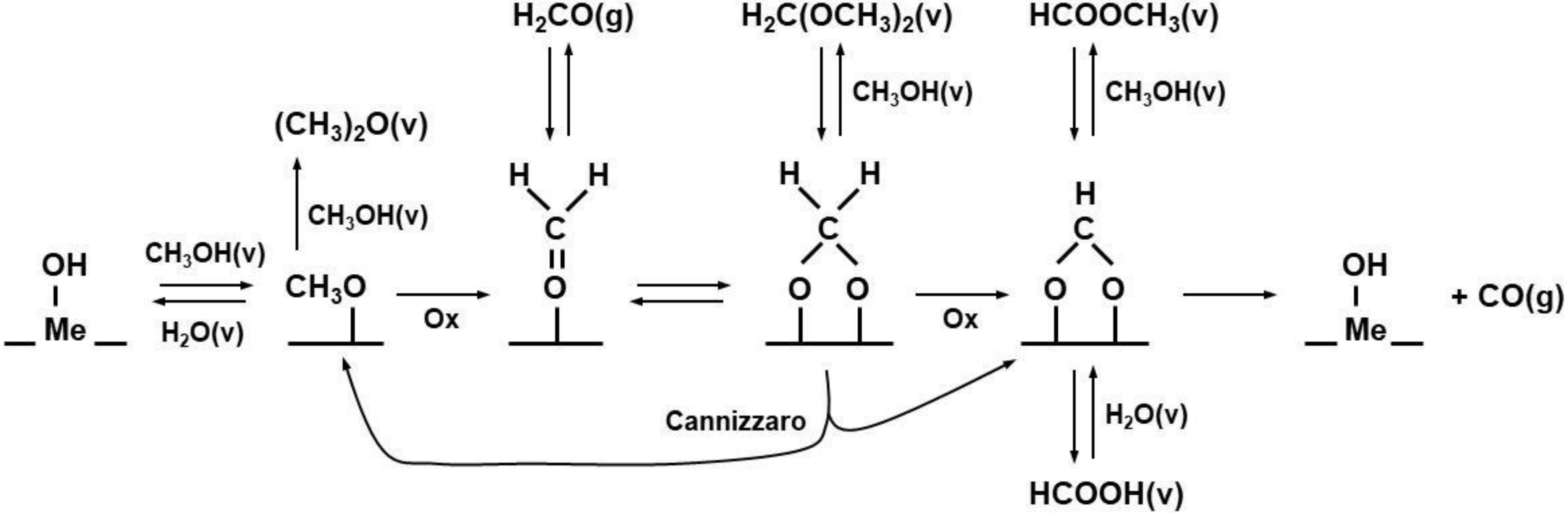

Scheme S1. Methanol oxidation reaction pathways (rake mechanism) depending on the strength of acidic centers established by Busca et al. [G. Busca, A. S. Elmi and P. Forzatti, *J. Phys. Chem.*, 1987, **91**, 5263–5269].